Correction of the Solar Azimuth Discontinuity at Sunrise and Sunset

Harry D. Kambezidis [1,2], Konstantinos Mimidis [2], and Kosmas A. Kavadias [2]

[1]IERSD*, National Observatory of Athens, Athens, Greece
[2]DME**, University of West Attica, Athens, Greece
* Institute of Environmental Research and Sustainable Development
** Department of Mechanical Engineering

E-mail: harry@noa.gr

Accepted: 18 June 2020

***Abstract*:** Solar azimuth may become indefinite at sunrise and sunset. This discrepancy is corrected in the present work. The correction concerns application of Fourier–series analysis to the solar paths over a site during days when the problem arises. The result is the derivation of a new curve that is fitted with great accuracy to the daily solar azimuth values, thus bridging the gap of the discontinuity. A demonstration for the solar azimuth correction is given for 3 sites around the world (Athens, Stockholm, and Sydney). The correction can be applied to any solar geometry code; in this work the algorithm of the XRONOS code is selected without (XRONOS.bas, a BASIC programme) and with (XRONOS.m, a MATLAB code) the correction proposed. A corrected expression for the atmospheric refractive index at various altitudes is given in Appendix A as the refraction of solar right is treated in XRONOS

Keywords: solar azimuth, sunrise, sunset, discontinuity, SUNAE, XRONOS.

1. Introduction

An exact estimation of the position of the sun in the sky at any location on earth is a prime task for any solar radiation scientist or solar energy engineer. This occurs because solar radiation is required to be estimated via modelling most of the time due to the scarcity of solar radiation measuring stations worldwide (Katiyar & Pandey, 2013). The exact position of the sun in the sky is a key parameter for an accurate estimation of its instantaneous intensity, which, in turn, may result in an accurate assessment of the solar potential at the location after integrating the instantaneous values over time (e.g., hours, months or years).

To calculate the solar position in the sky, various algorithms have been developed. These algorithms are either in the form of an on-line tool (e.g., the Sun Path Chart available at http://solardat.uoregon.edu/SunChartProgram.php, the Sun Position Calculator available at https://www.volker-quaschning.de/datserv/sunpos/index_e.php, or the Logiciel CalSol in the French language available at http://ines.solaire.free.fr) or in the form of a code; such codes are the SUNAE algorithm (Walraven, 1978) and its modifications (Walraven, 1979; Archer, 1980; Muir, 1983; Wilkinson, 1983), which resulted in the renamed XRONOS code (Kambezidis and Papanikolaou, 1990; Kambezidis and Tsangrassoulis, 1993); also, the SPA code (Reda and Andreas, 2004), the PSA code (Blanco-Muriel et al., 2001), the ENEA code (Grena, 2008), the Michalsky algorithm (Michalsky, 1988), and the 1971 Spencer calculations. Recently, Zhang et al., (2021) proposed a new mathematical formula, which introduces the notion of the sub-polar point and calculates the solar vector.

The accuracy of the various tools and algorithms varies. The present work focuses on those codes that are applications running on a PC. The Spencer formula has a maximal error

DOI:10.31401/SunGeo.2022.01.04

greater than 0.25°, later reduced to 0.02°. The SUNAE had an error of 0.013° reduced to 0.001° in XRONOS; the Michalsky algorithm has the disadvantage of time limitation in the accuracy of calculations (1950-2050), while the PSA code works correctly for the period 1995-2015. The SPA code has a maximum error of 0.008°, while the ENEA one of less than 0.0003°, but its cost is complexity as it requires a large number of intrinsic calculations. Therefore, it seems that the XRONOS code, though a simple-to-use algorithm, provides sufficient accuracy to solar radiation modellers, and moreover to solar energy engineers. The XRONOS code is an embodied routine in the Meteorological Radiation Model (MRM, e.g., Kambezidis et al., 2000, 2017; Kavadias et al., 2014), as the MRM, as any solar radiation model, pre-requires the calculation of solar geometry before the estimation of the value of solar radiation. Nevertheless, recently a discontinuity error was detected in XRONOS regarding the calculation of solar azimuth at the moments of sunrise and sunset. This discontinuity is related to the analytical expressions that calculate the solar azimuth. The aim of the present study is, therefore, to provide corrected expressions for this parameter.

2. Description of the Discontinuity

The initial SUNAE algorithm was implemented as a FORTRAN programme (i.e., SUNAE.for). The modified SUNAE, which has been renamed to XRONOS (XRONOS means time in Greek, X is pronounced CH), was first implemented as a routine written in the BASIC programming language (i.e., XRONOS.bas). The recent correction to the solar azimuth was made in the MATLAB environment and, therefore, XRONOS is a MATLAB routine now (i.e., XRONOS.m).

The expressions for estimating the solar altitude, γ, and solar azimuth, ψ, at any moment over any location on earth are the following (Kambezidis, 2012):

$$\sin\gamma = \sin\varphi \cdot \sin\delta + \cos\varphi \cdot \cos\delta \cdot \cos\omega, \quad (1)$$

$$\sin\psi = \frac{\sin\gamma \cdot \sin\varphi - \sin\delta}{\sin\gamma \cdot \cos\varphi}, \quad (2)$$

where φ is the geographical latitude of the location given by the user, δ is the solar declination, and ω is the hour angle, all in degrees; γ varies in the range [-90°, +90°] with positive after sunrise and negative values after sunset (i.e., above and below the local horizon, respectively); ψ lies in the interval [-180°, +180°] with positive after and negative values before solar noon (i.e., ψ = 0° when the sun is over the local south of the observer); φ varies in the range [-90°, +90°] with positive in the northern and negative values in the southern hemisphere; δ is in the range [-23.5°, +23.5°] throughout the year, and ω varies in the interval [-90°, +90°] with positive after and negative values before solar noon (i.e., ω = 0° when the sun is over the local south of the observer). The analytical relationships for the calculation of δ and ω are (Walraven, 1978):

$$\sin\delta = \sin\varepsilon \cdot \sin LONG, \quad (3)$$

$$\omega = ra - s, \quad (4)$$

$$\varepsilon = 23.442 - 3.56x10^{-7} \cdot time, \quad (5)$$

$$time = (YEAR - 1980) \cdot 365 + int\left(\frac{YEAR - 1980}{4}\right) + DOY - 1 + \frac{t}{24}, \quad (6)$$

$$t = HOUR + \frac{MIN}{60} + ZONE, \quad (7)$$

$$s = st + 15 \cdot t - LONG, \quad (8)$$

$$st = 1.759335 + 2\pi \cdot \left(\frac{time}{365.25}\right) - (YEAR - 1980), \quad (9)$$

where ε is the angle between the ecliptic plane and the plane of the celestial equator (in degrees), and LONG, ZONE are the geographical longitude and time zone of the location, respectively, (in degrees, positive west and negative east of the Greenwich meridian) given by the user; the function int(…) delivers the integer value of the argument; DOY is the day of the year (1 for 1 January, 365, or 366, for 31 December in a non-leap, or leap, year), while the variables YEAR, HOUR, MIN are the year, hour, and minute for which the calculations are to be made and are provided by the user.

DOI:10.31401/SunGeo.2022.01.04

In the above equations, the atmospheric refraction has been neglected. Since this factor is important in the calculations of solar altitude (or solar elevation) and solar azimuth, this effect must be considered in Equation (1). Therefore, for more accurate estimation of the γ and ψ values the following expressions replace Equations (1) and (2) (Kambezidis & Papanikolaou, 1990):

$$\gamma = ets + ref, \quad (10)$$

$$\tan\psi = \frac{\theta}{\sqrt{|1 - \theta^2|}}, \quad (11)$$

$$\tan ets = \frac{1}{\sqrt{(1-q^2)}}, \; q = \sin\gamma, \quad (12)$$

$$ref = 3.5163977 \cdot \frac{0.1594 + 0.0196 \cdot ets + 0.00002 \cdot ets^2}{1 + 0.505 \cdot ets + 0.0845 \cdot ets^2}, \quad (13)$$

$$\theta = \frac{\cos\delta \cdot \sin\omega}{\cos\gamma}. \quad (14)$$

The above expressions give accurate values for γ and ψ. Nevertheless, the estimation of ψ at the moments of sunrise or sunset may deliver a discontinuity. Indeed, Equation (14) becomes indefinite (θ = ∞) when cosγ = cos(±90°) = 0. Therefore, Equation (11) presents a discontinuity in ψ because of θ = ∞.

To demonstrate the mentioned problem, use of the XRONOS code was made. Figure 1 deploys the solar path on 3 days of 2021 for Athens (i.e., the solar equinox of 21 March, the summer solstice of 21 June, and the winter solstice of 21 December). The discontinuities occur for values of ψ around -90° and +90°. For the winter solstice the discontinuities occur well before sunrise and well after sunset (i.e., below the local horizon); therefore, they do not affect any solar radiation estimations. On the contrary, the ψ discontinuities on the spring equinox (and moreover the autumn one, not shown here) are happening just about sunrise and sunset (i.e., the local horizon) and may create some problems in solar radiation calculations. As regards the summer solstice, the discontinuities occur well above the local horizon (i.e., well after sunrise or well before sunset) and create miscalculations. Figure 1 gives a schematic diagram in which the daily paths over Athens are depicted for the 3 selected days.

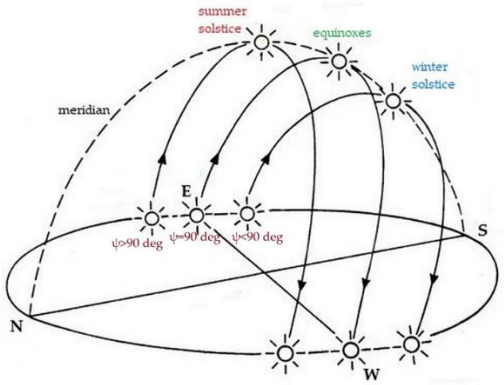

Figure 1. Daily paths of the sun in the sky of Athens on 21 June (summer solstice), during the equinoxes (21 March or 21 September), and on 21 December (winter solstice). N = north, S = south, E = east, W = west. The solar azimuth arc, ψ, measured from S on the local horizon, is less than, equal to, and greater than 90o at sunrise on the winter solstice, the two equinoxes, and the summer solstice, respectively. The indicated values of ψ are absolute ones because the minus sign (sign by convention to the east of the NS line) has been removed for easiness. The highest positions of the sun on the 3 paths refer to the 12:00 solar time (they lie in the meridian plane).

3. Correction of the Discontinuity

To overcome the discontinuity problem in solar azimuth calculations during the implementation of the XRONOS algorithm in particular, the Fourier-analysis methodology was applied to the problematic data time series.

The major advantage in applying a Fourier analysis to a data time series is that it can be used when a regression function cannot be established for the time series in question. In such cases, the unknown form of the data time series can be analysed and given in the form of sines and cosines. What is unknown since the beginning of the process is the optimum number of terms in the Fourier analysis that will effectively simulate the data time series. For the purpose of the present work, the lsqnonlin MATLAB routine was used. This function solves non-linear least-squares curve-fitting problems by minimising the square of the 2nd norm of the given function (i.e., the Fourier series). In the present study, a 6th-order Fourier-series function was eventually selected and used in XRONOS.m. Figure 2a is an

DOI:10.31401/SunGeo.2022.01.04

example of the solar azimuth discontinuities for the site of Athens observed at 16:30 LST during 2021. Figure 2b shows the result of applying the lsqnonlin routine to the solar azimuth data series and filling the discontinuity gaps.

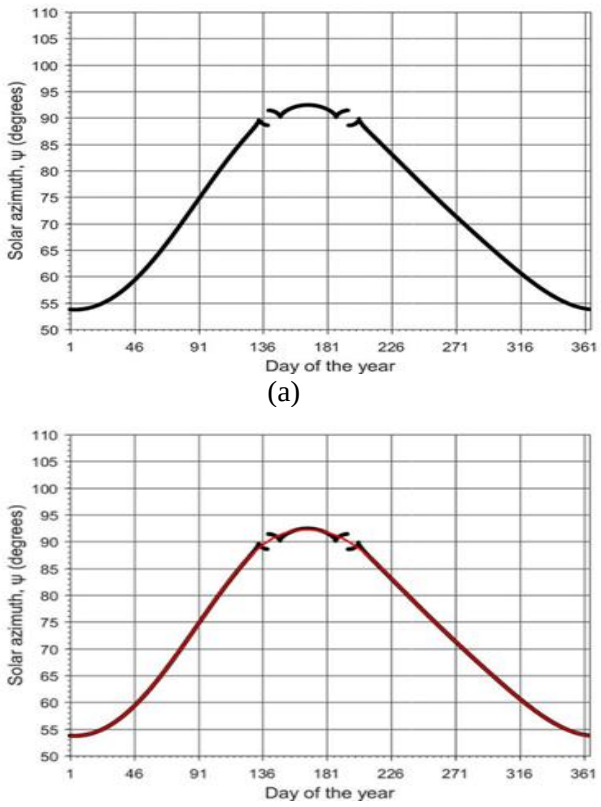

Figure 2. Solar azimuth values for Athens (φ = 37.96o N, λ = 23.71o E) at 16:30 LST within the year 2021; (a) discontinuities from XRONOS.bas, and (b) recovery of discontinuities from XRONOS.m (red line). N = northern hemisphere, E = east of the Greenwich meridian, φ = geographical latitude (LAT in XRONOS.m), λ = geographical longitude (LONG in XRONOS.m).

For a complete picture of the solar azimuth discontinuities, Figure 3 shows them in the form of annual solar analemmas for 3 selected sites in the northern and southern hemisphere. These analemmas were derived by using the XRONOS.bas algorithm providing the hourly values of γ and ψ for the whole 2021. On the contrary, Figure 4 shows smooth yearly solar analemmas for 2021 after implementing the lsqnonlin routine in the XRONOS.m algorithm for the above 3 cities.

3. Conclusions

The present work identified the problem of discontinuities in estimating solar azimuth. The discontinuity occurs on any day of the year at instances after sunrise or before sunset when ψ

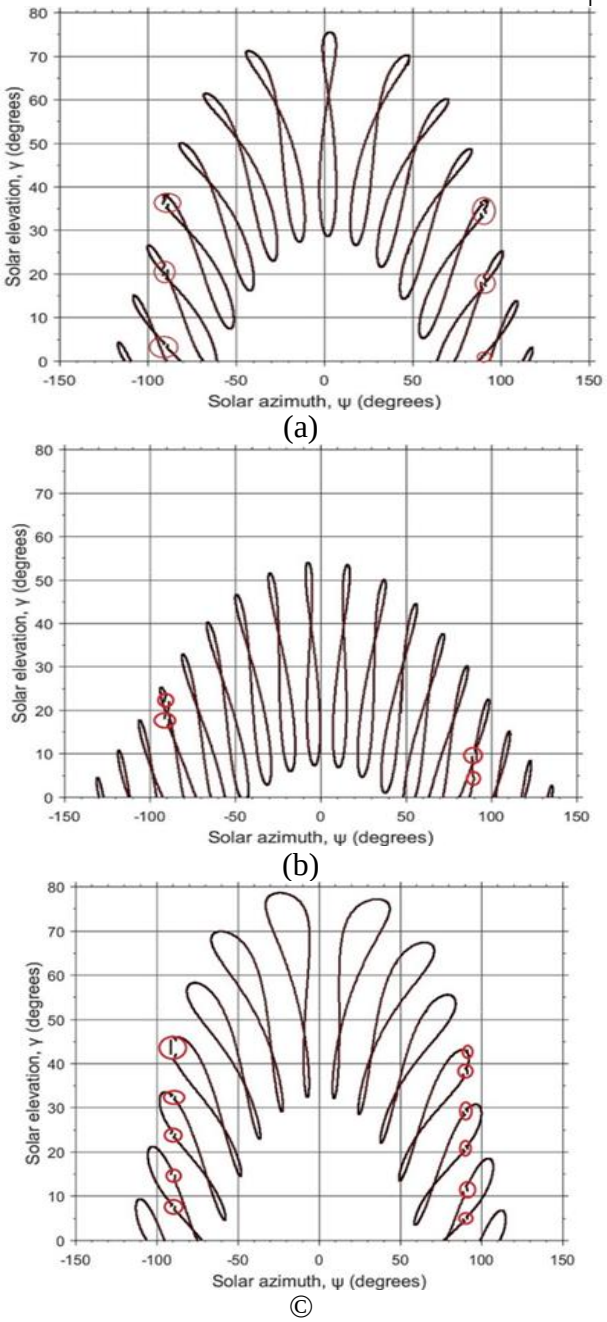

Figure 3. Solar analemmas for the year 2021 over (a) Athens (φ = 37.96o N, λ = 23.71o E), (b) Stockholm (φ = 59.32o N, λ = 18.07o E), and (c) Sydney (φ = 33.86o S, λ = 151.19o E) by using XRONOS.bas. The red circles show the solar azimuth discontinuities at ψ = ±90o. N = northern hemisphere, S = southern hemisphere, E = east of the Greenwich meridian, φ = geographical latitude (LAT in

DOI:10.31401/SunGeo.2022.01.04

XRONOS.m), λ = geographical longitude (LONG in XRONOS.m).

is equal to ±90^o. The problem was explained by analytical expressions and diagrams. The solution to the discontinuities was provided by

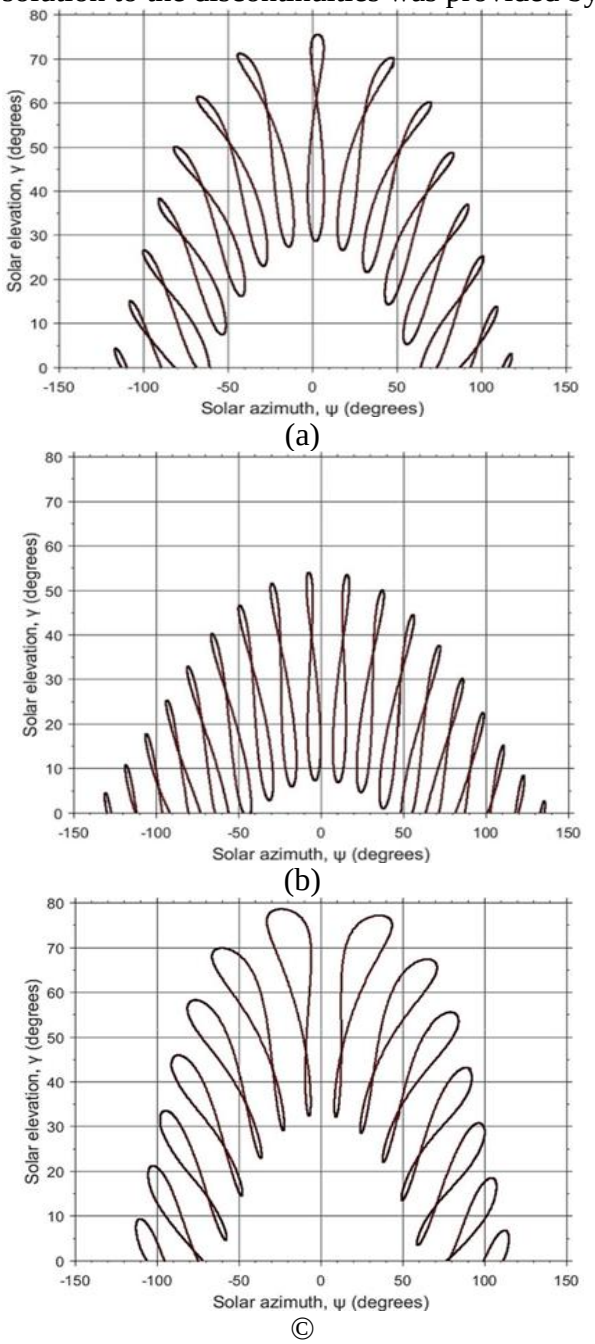

Figure 4. Solar analemmas for the year 2021 over (a) Athens (φ = 37.96o N, λ = 23.71o E), (b) Stockholm (φ = 59.32o N, λ = 18.07o E), and (c) Sydney (φ = 33.86o S, λ = 151.19o E) by using XRONOS.m. No analemma discontinuities are now observed at ψ = ±90o. N = northern hemisphere, S = southern hemisphere, E = east of the Greenwich meridian, φ = geographical latitude (LAT in XRONOS.m), λ = geographical longitude (LONG in XRONOS.m).

applying a Fourier-series analysis to the whole daily path of the sun on the day under question and by deriving a smooth curve without discontinuities.

The issue was demonstrated for 3 sites in the northern and southern hemisphere (i.e., Athens, Stockholm, and Sydney); for these cities, solar analemmas for 2021 were produced with and without discontinuities in ψ by using the XRONOS.bas and XRONOS.m algorithms, respectively.

Further, the corrected expressions for the atmospheric refraction, ref, used in the XRONOS.m algorithm are provided in Appendix A.

References

Archer, C. B.: 1980, Solar Energy 25(1), 91. https://doi.org/10.1016/0038-092X(80)90410-7

Berberan-Santos, M. N., Bodunov, E. N., and Pogliani, L.: 1997, American J. of Physics 65(5), 404. https://doi.org/10.1119/1.18555

Blanco-Muriel, M., Alarcón-Padilla, D. C., López-Moratalla, T., and Lara-Coira, M.: 2001, Solar Energy 70(5), 431.

Gipe, P. (2016). *Wind energy for the rest of us: A comprehensive guide to wind power and how to use it*. Wind-works.

Grena, R.: 2008, Solar Energy 82(5), 462. https://doi.org/10.1016/j.solener.2007.10.001

Kambezidis, H.D.: 2012, The solar resource. In Comprehensive Renewable Energy (Vol. 3). https://doi.org/10.1016/B978-0-08-087872-0.00302-4

Kambezidis, H.D., and Papanikolaou, N. S.: 1990, Solar Energy 44(3). https://doi.org/10.1016/0038-092X(90)90076-O

Kambezidis, H.D., Psiloglou, B. E., Karagiannis, D., Dumka, U. C., and Kaskaoutis, D. G.: 2017, Renewable and Sustainable Energy Reviews 74, 616. https://doi.org/10.1016/j.rser.2017.02.058

Kambezidis, H.D., and Tsangrassoulis, A. E.: 1993, Solar Energy 50(5). https://doi.org/10.1016/0038-092X(93)90062-S

Kambezidis, Harry D., Adamopoulos, A. D., Sakellariou, N. K., Pavlopoulos, H. G., Aguiar, R., Bilbao, J., de Miguel, A., and Negro, E.: 2000, in 1999 ISES Solar World Congress, p. 406. https://doi.org/10.1016/b978-008043895-5/50061-8

Karttunen, H., Kröger, P., Oja, H., Poutanen, M., and Donner, K. J.: 2016, Fundamental Astronomy, Springer Berlin Heidelberg. https://doi.org/10.1007/9783662530450

Katiyar, A. K., and Pandey, C. K.: 2013, Journal of Renewable Energy 2013, 1. https://doi.org/10.1155/2013/168048

Kavadias, K. A., Paliatsos, A. G., Kambezidis, H. D., & Bartzokas, A. (2014). Comparison of long-term broadband model results with experimental measurements. *Fresenius Environmental Bulletin*, *23*(12), 3178–3187.

DOI:10.31401/SunGeo.2022.01.04

Lunde, P. J.: 1980, Solar thermal engineering: space heating and hot water systems, Wiley. https://linkinghub.elsevier.com/retrieve/pii/0038092X83902128

Michalsky, J. J.: 1988, Solar Energy 40(3), 227. https://doi.org/10.1016/0038-092X(88)90045-X

Muir, L. R.: 1983, Solar Energy 30(3), 295. https://doi.org/10.1016/0038-092X(83)90164-0

Reda, I., and Andreas, A.: 2004, Solar Energy 76(5), 577. https://doi.org/10.1016/j.solener.2003.12.003

Walraven, R.: 1978, Solar Energy 20(5), 393. https://doi.org/10.1016/0038-092X(78)90155-X

Walraven, R.: 1979, Solar Energy 22(2), 195. https://doi.org/10.1016/0038-092X(79)90106-3

Wilkinson, B. J.: 1983, Solar Energy 30(3), 295. https://doi.org/10.1016/0038-092X(83)90165-2

Zhang, T., Stackhouse, P. W., Macpherson, B., and Mikovitz, J. C.: 2021, Renewable Energy 172, 1333. https://doi.org/10.1016/j.renene.2021.03.047

Appendix A

This section provides a discussion about Equation (13), which calculates the atmospheric refraction effect on solar altitude. Unfortunately, this expression assumes that the solar geometry calculations are made for sites at sea level or even low-level altitudes. For sites at high altitudes (above ≈200 m asl, asl = above sea level), the calculations may be erroneous because lower and lower air density with altitude results in more and more bending of the solar rays. This effect has not been accounted for in Equation (13). Therefore, this section refers to this correction, which is implemented in the XRONOS.m algorithm.

According to Karttunen et al. (2016) the expression for the atmospheric refraction, ref, at various altitudes, z (in m asl), is given by the equations:

$$ref = \frac{P_z \cdot 0.00452 \cdot \tan(90-\gamma)}{273+T_z}, \text{ for } \gamma > 15^o \quad \text{(A1a)}$$

$$ref = \frac{P_z \cdot (01594+0.0196 \cdot \gamma+0.00002 \cdot \gamma^2)}{(273.15+T_z) \cdot (1+0.505 \cdot \gamma+0.0845 \cdot \gamma^2)}, \text{ for } \gamma \le 15^o \quad \text{(A1b)}$$

where P_z is the barometric pressure (in hPa), and T_z the air temperature (in ^{o}C) at altitude z. An alternative expression to Equations (A1a) and (A1b) is by replacing the coefficient 3.5163977 in Equation (13) with the ratio P_z/T_z; the new expression for ref is, therefore, the following and this is used in XRONOS.m:

$$ref = \frac{P_z}{T_z} \cdot \frac{0.1594+0.0196 \cdot ets+0.00002 \cdot ets^2}{1+0.505 \cdot ets+0.0845 \cdot ets^2}. \quad \text{(A2)}$$

It should be noted here that the coefficient 3.5163977 in Equation (13) is just the ratio $P_0/T_0 = 1013.25/288.15 \approx 3.5163977$ hPa·K^{-1}, which calculates ref at sea level.

Equation (A2) requires the knowledge of P_z and T_z. If these values cannot not be found or retrieved, then use of the following approximate formulas can be made (Gipe, 2016).

$$P_z = P_0 \cdot \left(\frac{T_0 - T_z}{T_0}\right)^{\frac{g}{R}}, \quad \text{(A3a)}$$

$$R = \frac{6.5 \cdot z}{1000}, \quad \text{(A3b)}$$

where P_0 is the baromatric pressure at sea level (taken as 1013.25 hPa or sometimes 1000 hPa), g is the acceleration due to gravity (equal to ≈9.81 m·s^{-2}), T_0 is the air temperature at sea level (equal to 288.15 K), T_z is the air temperature at altitude z, and R is a scaling factor that takes into account the adiabatic lapse rate of 6.5 ^{o}C per 1000 m altitude.

If the estimation of P_z and T_z would be to be avoided, then use of the following approximate calculations can be made (Lunde, 1980; Berberan-Santos et al., 1997; Karttunen et al., 2016). These expressions were used in XRONOS.m for deriving the results in Figs. 4a,b,c, because of unknown values of P_z and T_z at the 3 sites.

$$P_z = P_0 \cdot e^{-\frac{z}{8435.2}}, \quad \text{(A4a)}$$

$$T_z = \frac{6.5 \cdot z}{1000} + T_0. \quad \text{(A4b)}$$

DOI:10.31401/SunGeo.2022.01.04